

## **Properties of Binary and Ternary Composites of Polypropylene containing Soybean Oil-g-Chitosan and Hydrophobic Phosphonated Silica**

**Natthaphop SUWANNAMEK<sup>1</sup> and Kawee SRIKULKIT<sup>1,2\*</sup>**

<sup>1</sup> *Department of Materials Science, Faculty of Science, Chulalongkorn University, Bangkok, 10330, Thailand*

<sup>2</sup> *Center of Excellence on Petrochemical and Materials Technology, Chulalongkorn University, Bangkok 10330, Thailand*

### **Abstract**

PP/soybean oil-g-chitosan binary composite, PP/hydrophobic phosphonated silica binary composite, and PP/chitosan/hydrophobic phosphonated silica ternary composite were prepared. Firstly, the preparation of soybean oil-g-chitosan was carried out by surface hydrophobicity modification of chitosan powder with soybean oil maleate and hydrophobically phosphonated silica was prepared by silanization of phosphonated silica with hexadecyltrimethoxysilane (an organosilane). Binary and ternary composites were prepared using a twin screw extruder. It was found that soybean oil-g-chitosan not only caused a decrease in tensile strength but also enhanced flexibility of PP due to its plasticization effect. In the opposite direction, the addition of hydrophobic phosphonated silica resulted in an increase in tensile modulus and a decrease in percent elongation at break due to reinforcement characteristic of silica particle. Effects of soybean oil-g-chitosan and phosphonated silica on antimicrobial activity and flame retardancy property, respectively, were evaluated. Results showed that binary PP composites containing soybean oil-g-chitosan exhibited antimicrobial performance when compared to neat PP. For binary composite containing phosphonated silica, flame resistance was improved which was indicated by relative char content. An addition of soybean oil-g-chitosan led to phosphorus-nitrogen synergism effect (70% of remaining residue weight at T 450°C) as found in case of ternary composite containing 1 wt% soybean oil-g-chitosan and 1 wt% phosphonated silica.

**Keyword:** Soybean oil-g-chitosan; Hydrophobic phosphonated silica; Polypropylene composites; Antimicrobial; Flame retardancy.

**DOI:** 10.14456/jmmm.2015.5

### **Introduction**

Polypropylene (PP) is one of commodity plastics commonly found in many end-use products due to advantageous properties such as light weight, resistance to moisture and chemicals, low cost, sufficient strength and ease of processing. However, PP has some disadvantages particularly poor impact strength at low temperature and sensitivity to light and heat. Loading of fibers (natural fiber, glass fiber or synthetic organic fibers such as carbon fiber, PET fiber, and kevlar) into PP matrix was found to improve the PP tensile strength and toughness<sup>(1-5)</sup>. On the other hand, addition of inorganic fillers such silica can enhance the thermal property as well as stiffness but at an expense of the toughness<sup>(6)</sup>.

Preparation of ternary composites was found to solve these drawbacks. Recently, the demand for greater value goods has been a driving force to develop specialty products based on commodity polymers. Functional properties such as flame retardancy and antimicrobial activity are interesting since PP is lack of these properties. By preparation of ternary composites, their functional properties can possibly be imparted into PP by the addition of functional fillers such as chitosan (antimicrobial agent) and phosphonated silica (flame retardant).

Chitosan having the degree of deacetylation (%DD) more than 80% can be obtained by the deacetylation of chitin. Chitosan exhibits excellent biocompatibility, biodegradability, and non-toxicity with versatile biological activities including antimicrobial activity. Hence, chitosan is of great interest in terms of wide range of applications. Its antimicrobial property is related to the interaction.

---

\* Corresponding author Email: ksriulkit@gmail.com

of charges between the amino groups of the polycationic form of chitosan with the microbial cell walls. The degradation of proteins and other intracellular constituents then occur, as well as alterations on the permeability of the microbial cell, which induces the loss of essential nutrients and eventually death<sup>(7)</sup>. Due to the nature of chitosan which is a nitrogen-containing polymer, the co-application of chitosan powder with phosphonated silica into PP was anticipated to enhance the formation of intumescent char, therefore imposing the anti-dripping effect<sup>(8,9)</sup>.

Based on the polymer composite approach, flame retardancy can be achievable. Flame retardancy effect is the characteristic of self-extinguishing when the ignition source is removed. There are many flame retardant additives such as endothermic additives (metal hydroxide), halogenated flame retardant, antimony trioxide, phosphorus additives, expandable graphite, hindered amines, nanocomposite, silicone, etc.<sup>(10-14)</sup>. Commercially flame retardants are mostly employed as systems consist of several components. The benefits of synergistic effects are particularly taken into consideration. Synergism means that the overall flame retardancy effect is higher than the sum of the single components effects. Many synergistic systems based on phosphorous and nitrogen, metal hydroxides and salts have been developed in recent years. Examples are the synergy between metal phosphinates and melamine polyphosphate, as well as aluminum oxide hydrate (bohemite) or melamine polymetal phosphates<sup>(15-17)</sup>.

Phosphorus flame retardants (PFRs) function in two ways. In the first manner, volatile PFRs react with each other or other compounds and then become volatile or solid phase upon the burning materials. In another aspect, the flame inhibitions slowdown the oxidation and make an incomplete combustion zone which reduces the flammable time period<sup>(10)</sup>. PFRs act in the solid phase when heated phosphorous compounds release a polymeric form of phosphoric acid. This acid causes the material to char, forming a glassy layer of carbon, and thus inhibiting the "pyrolysis" process which supplies fuel to the flame<sup>(18)</sup>. The char acts as a two-way barrier, both obstructing the path of the combustible gases towards the flame and protecting the polymer from the heat. Furthermore, this mode of action significantly reduces the amount of fuel produced which is protected by the formed char. Certain products contain both phosphorus and chlorine or nitrogen, thus combining the different flame retarding mechanisms of these elements. Additive phosphorus-containing flame retardants can simply

be mixed into the plastics by a melt mixing machine.

Phosphorus compound can be divided into 6 categories : alkyl - phosphates, aryl - phosphates, bisarylphosphates, red phosphorus, ammonium polyphosphate (APP), and others<sup>(17)</sup>. Alkyl-phosphates or halogenated phosphate esters are manufactured by the reaction of alkylene oxides and phosphorous chlorides. Chlorinated phosphate esters are widely used for polyurethane foams in range of 5-15% loading. Aryl-phosphates are synthesized by phosphorous oxychloride and phenols or mixture of phenols and alcohols. The commercial products are triphenylphosphate (TPP), isodecylphosphate (IDP), bis-(tert-butylphenyl) phenylphosphate (BBDP), etc. Arylphosphates as plasticizers are widely used in PVC products. Bisarylphosphates are made from the reaction of phosphorus oxychloride and various phenols. However, phosphorus based flame retardants are not suitable for melt processing process particularly olefin polymers which are required extremely high amount of loading to impart effective flame retardancy. The high amount of loading imposes the processing difficulty and deteriorates the mechanical properties. Polymer nanocomposites could potentially be a solution to this disadvantage. A nanocomposite is a multiphase solid material where one of the phases has one, two or three dimensions of less than 100 nanometers (nm), or structures having nano-scale repeat distances between the different phases that make up the material. Polymer nanocomposites (PNC) consist of a polymer or copolymer having nanoparticles or nanofillers dispersed in the polymer matrix. Researches on nanocomposites having flame retardants were reported. The dispersibility effect of nanomagnesium hydroxide (nano-MH) on the flammability of ternary composites was studied<sup>(18)</sup>. Polymer/crosslink rubber/nano-magnesium hydroxide ternary composite was prepared by co-spray drying technique. The uniform dispersion of nano-MH can enhance the flame retardancy compared with the conventional mixing method. It was found that fumed silica exhibited flame retardancy and had a synergistic effect with MH in the EVA/MH/SiO<sub>2</sub> blends<sup>(19,20)</sup>. In addition, clay or phyllosilicate was also applied as flame retardant materials. The addition of nanodispersed montmorillonite (MMT) clay in polymeric matrices which produced a substantial improvement in fire performance was published<sup>(21)</sup>.

In this study, PP/soybean oil-g-chitosan binary composite, PP/phosphonated silica binary composite, and PP/chitosan/phosphonated silica ternary composite were prepared using a twin screw extruder. The preparation of soybean oil-g-chitosan

was carried out by surface hydrophobicity modification of chitosan powder with soybean oil maleate and hydrophobically phosphonated silica was prepared by silanization of phosphonated silica with an organosilane. Characterizations and properties evaluation of binary and ternary composites were performed and discussed.

## Materials and Experimental Procedures

### Materials

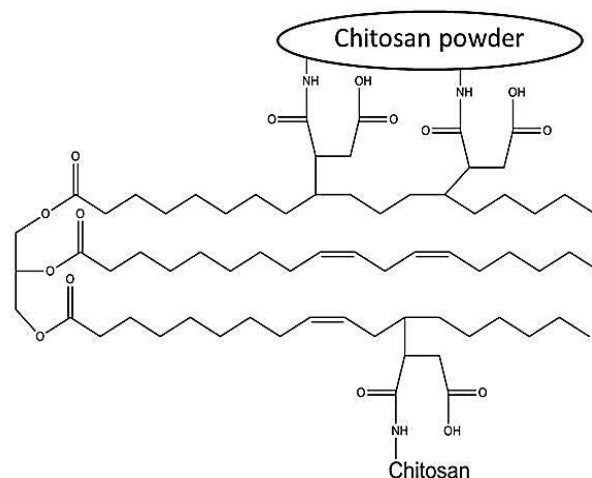
Commercial-grade chitosan flake with a molecular weight of about 106 Da was purchased from ANN lab, Thailand. Commercial-grade methanol was purchased from TSL Chemical (Thailand) Co., Ltd. and distilled prior to use. Soybean oil maleate was synthesized according to the previous report<sup>(22)</sup>. Phosphorus acid and 40% (w/v) formaldehyde were purchased from Aldrich (Germany). Toluene purchased from local supplier was distilled before use. Hexadecyltrimethoxysilane (HDTMS, Dynasylan 9116) and fumed silica (AEROSIL200) having an average particle size of 14 nm and surface area of 200 m<sup>2</sup>/g were kindly provided by Evonik. Aminopropyltriethoxysilane (APTES) was purchased from Shin-Etsu Silicaone (Japan). Polypropylene chip (MFI = 25g/10 min, density 0.9 g/cm<sup>3</sup>) was bought from HMC Polymers (Thailand).

### Synthesis of Soybean Oil-g-Chitosan

Chitosan powder was prepared as follows: 5 g of chitosan flakes was dissolved in 2 L of 0.2 M acetic acid solution and followed by precipitating chitosan by addition of 15 ml of 1 M NaOH. The precipitated chitosan was filtered and neutralized. Then, DI water was added to the neutralized precipitated chitosan at 1:1 weight ratio. The slurry was fed to spray dryer (HVAC model SD-01, Thailand) at 20L/h, inlet temp 170°C, outlet temp 90°C and nozzle pressure of 1.5 bar. The chitosan powder was collected.

Soybean oil-g-chitosan (SB, Figure 1) was prepared by reaction of spray dried chitosan powder with soybean oil maleate. 50 g soybean oil maleate and 50 g chitosan powder at actual weight ratio of 1:1 were well mixed using a mechanical stirrer. Small amount of acetone was added to reduce the viscosity of soybean oil maleate. After that, the mixture was put into the hot-air oven set the temperature at 80°C for 2 hours. Then, the crude product was washed with acetone to remove

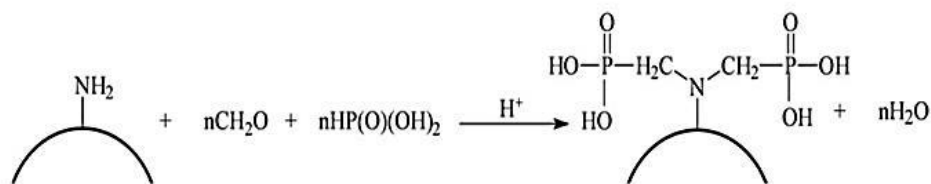
unreacted soybean oil maleate. The resultant SB was dry when left standing at room temperature for 24 h.



**Scheme 1.** The schematic structure of soybean oil-g-chitosan

### Synthesis of HDTMS-g-Phosphonated Silica

The attachment of amino groups onto silica particle surface was achieved by a silanization reaction between the surface AEROSIL200 silanol groups and APTES silane group. The reaction was performed in a 600-mL flask containing 15.0 g AEROSIL200 and 500 mL toluene as reaction medium. The mixture was continuously stirred by a magnetic stirrer for 30 min. Then 50 mL of methanol: water mole ratio of 2:1 was added to the mixture and stirred for 72 h.<sup>(23)</sup> After that, the APTES silica particles were filtered and extracted with toluene for 24 hours using a Soxhlet extractor to remove the unreacted APTES. The APTES-treated silica was dried in an oven at 60°C for 24 h and stored in a desiccator. Then, APTES-treated silica, crystalline phosphorous acid, concentrated hydrochloric acid, and H<sub>2</sub>O were mixed in a total volume of 200 mL dispersion and, then, the mixture was heated to reflux in a three-necked flask fitted with thermometer, condenser and dropping funnel. Over the course of about 1 hour, 60 mL of a 40% (w/v) aqueous formaldehyde solution was added drop by drop, and the reaction was kept at the reflux temperature for an additional hour. The product was neutralized with concentrated ammonia solution and followed by precipitation in methanol. The representative mechanism of this reaction (Mannich type reaction) is given in Scheme 2.



Scheme 2. Synthesis of phosphonated silica involving aminopropyl triethoxysilane-treated silica, formaldehyde, and phosphorus acid<sup>(23)</sup>.

Phosphonated silica particle surface was then hydrophobically modified by hexadecyltrimethoxysilane (Dynasylan 9116). Phosphonated silica (100 g) was dispersed in 100 ml hexadecyltrimethoxysilane emulsion prepared by using 1000 ml of 0.1 wt% nonylphenol ethoxylate surfactant and 100 g of hexadecyltrimethoxysilane. Then, 50 ml methanol was added to the dispersion under vigorous stirring. pH value was adjusted to pH 1 by addition of diluted HCl. The mixture was left standing for 3 days to allow the complete silanization reaction. The wet cake of HDTMS treated phosphonated silica was dried at 60°C for 24 hours to obtain white fluffy silica powder prior to the preparation of binary and ternary composites.

*Preparation of PP/Soybean Oil-g-Chitosan(SB) binary composite and PP/HDTMS-Phosphonated silica(P) and PP/Soybean Oil-g-Chitosan/HDTMS-Phosphonated Silica Ternary composite*

Polypropylene / 10 wt% SB masterbatch and Polypropylene / 20 wt% P masterbatch were prepared by a twin-screw extruder using corrotating mode. The processing parameters including barrel zone temperatures 200-225 °C and screw speed (100 rpm/min) were optimized to obtain homogenous mixing. The composite samples were prepared by injection machine, FANUC model S-2000i100B to form bar and dog bone shapes samples. The formulation of polymer composites employed in this experiment was given in Table 1

Table 1. Compositions of the composites (weight ratio).

Sample	1	2	3	4	5	6	7	8	9	10	11	12	13
PP	99.75	99.50	99.00	98.00		99.50	99.00	98.50	99.00	98.50	98.50	980	100.00
Phosphonated silica (P)						0.50	1.00	1.50	0.50	1.00	0.50	1.00	
Soybean oil-g-chitosan (SB)	0.25	0.50	1.00	2.00					0.50	0.50	1.00	1.00	

### Characterizations and Testings

FTIR analysis was carried out using Perkin Elmer Spectrum One FT-IR spectrometer. Spectra were recorded in transmission mode from 550 cm<sup>-1</sup> to 4000 cm<sup>-1</sup> with 32 acquisitions and 4 cm<sup>-1</sup> resolution. The sample morphology was examined using scanning electron microscope (JEOL JSM-6510). Micrographs of the cross/crack sections of the sample were taken to evaluate the dispersion and agglomeration of the filler phase in the matrix.

Tensile properties were measured according to ASTM Standard D638: Standard Test Method for Tensile Properties of Plastic. The specimen from the Fanuc S-200i100B injection machine with plastic injection mold according to type V dimensions. Tensile strength test was conducted using Lloyd LR 10K plus

series with 10 kN and the specimens ruptured between 30 and 300 s. Izod impact energy was tested according to ASTM Standard D4812: Standard Test Method for Unnotched Cantilever Beam Impact Resistance of Plastic. The unnotched specimen was struck by a swinging pendulum on CEAST impact tester machine.

The thermal degradation characteristics of binary and ternary composites were determined by thermal gravimetric analyzer (Nicolet 6700, Thermo scientific) recorded in the temperature ranging from 30 to 600°C with a heating rate of 10°C/min.

Flame retardancy testing was performed with horizontal burning test according to ASTM D635: Standard Test Method for Rate of Burning and/or Extent and Time of Burning of Plastic in a Horizontal Position and recorded with a camera monitor.

Antimicrobial activity was evaluated according to method AATCC Test Method 100-1999 using *Staphylococcus aureus* and follow a standard dilution technique<sup>(24)</sup>. The percent microbial reduction and viability are presented.

## Results and Discussion

### Characterizations of Soybean Oil-g-Chitosan and HDTMS-g-Phosphonated Silica

FTIR spectra of chitosan and soybean oil-g-chitosan are presented in Figure 1. From the figure, soybean oil-g-chitosan exhibits the absorption bands at  $1849\text{ cm}^{-1}$ , corresponding the ester bonding formed by the ring opening reaction between soybean oil maleate anhydride group and chitosan amino group<sup>(22)</sup>. In addition, the peak intensity in the region of  $1560\text{--}1660\text{ cm}^{-1}$  assigned to amino groups decreases due to the reaction. As a result, chitosan powder surface is turned to be hydrophobic due to the coverage of soybean oil moiety. Furthermore, the hindered hydrophilicity is witnessed by the broadly weak intensity of hydroxyl bands between  $3000\text{--}3500\text{ cm}^{-1}$  when compared to the spectrum of virgin chitosan. It is anticipated that soybean oil-g-chitosan powder exhibits good dispersibility in PP matrix when compared to virgin chitosan

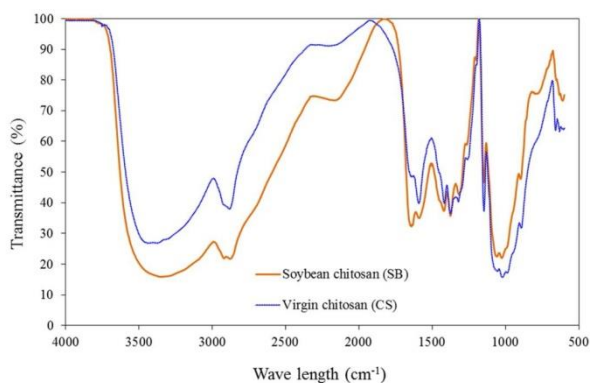


**Figure 1.** FTIR spectra of chitosan (CS) and soybean oil-g-chitosan (SB).

### Morphology of filler particles

SEM images of soybean oil-g-chitosan powder and spray dried chitosan powder are compared as shown in Figure 2. Spherical particles with average sizes between  $5\text{--}10\ \mu\text{m}$  were obtained. Before and after treatment, the appearance of chitosan surface remains unchanged. Interestingly, the average particle size of soybean oil-g-chitosan powder is relatively smaller than spray dried chitosan powder.

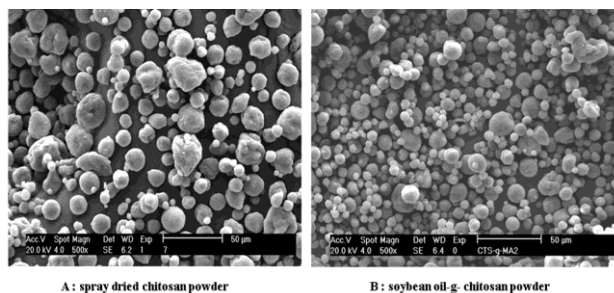


**Figure 2.** SEM images of spray dried chitosan powder (A) and soybean oil-g-chitosan (B)

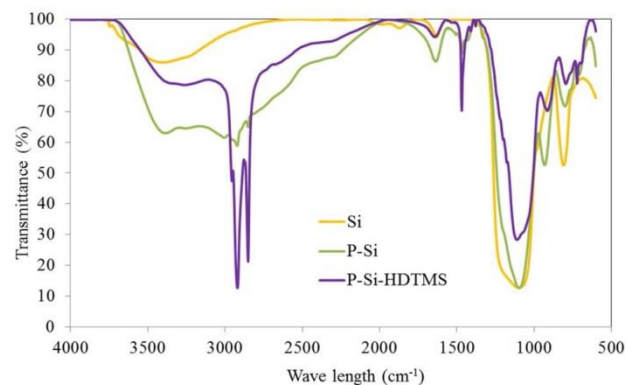


**Figure 3.** FTIR spectra of Silica, Phosphonated silica, and HDTMS-phosphonated silica.

Figure 3 compares FTIR spectra of silica, ATPES-silica, phosphonated silica, and HDTMS-phosphonated silica. Silica exhibits strong absorbance band around  $1,200\text{ cm}^{-1}$  and  $3,200\text{--}3,400\text{ cm}^{-1}$  which are corresponding to the siloxane (Si-o-Si) and silanol (-Si-OH) bands, respectively<sup>(25)</sup>. In contrast, HDTMS-phosphonated silica obviously exhibits the hydrophobicity characteristic which is indicated by the presence of hydrophobic long alkyl chain appearing between  $2,900\text{ cm}^{-1}$  and  $3,000\text{ cm}^{-1}$ . In addition, silanol bands between  $3,200\text{ cm}^{-1}$  and  $3,400\text{ cm}^{-1}$  completely disappear from spectrum of HDTMS-phosphonated silica<sup>(26)</sup>.

### Morphology of Binary and Ternary Composites

Commonly, there are two types of fracture found when polymeric materials are subject to forces: ductile fracture and brittle fracture. For typical polypropylene, brittle fracture is dominant. In this experiment, the fractured surface of polypropylene composite observed by SEM is presented in Figure 4. As seen, the smooth surface of fractured neat PP with straight line cracks is observed, indicating the brittleness characteristic of PP. In contrast, SEM images of PP/SB composites and PP/SB/P composites show rough fracture surface which is indicative of ductile fracture behavior. At the magnification of 1500X, SEM images reveal that

filler particles in the range between 0.25 and 1 wt% loading, are not detectable, implying that filler sizes are very fine. In addition, the problem of particle agglomeration does not exist. Hence, it was

anticipated that soybean oil-g-chitosan and HDTMS-phosphonated silica could affectively play their role in modifying mechanical properties of polypropylene including flexibility and stiffness

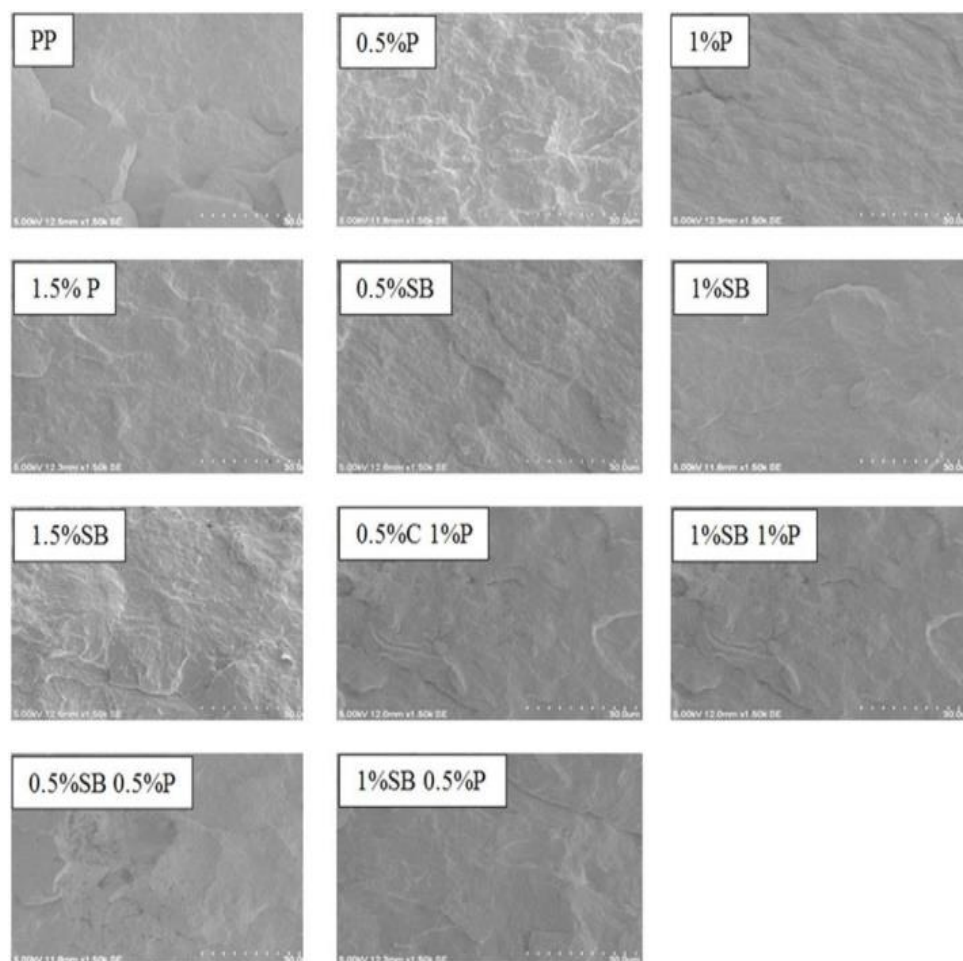


**Figure 4.** SEM images of fracture surface of binary and ternary composites.

#### *Mechanical Properties*

General mechanical properties (modulus, tensile strength and percent elongation at break) of binary and ternary composite representatives are presented in Figure 5-7. In case of PP/SB composites, the addition of soybean oil-g-chitosan causes a slight decrease in tensile strength. In the opposite direction, the elongation at break is found higher than that of neat PP. It is believed that both a decrease in tensile strength and an increase in percent elongation are influenced by the grafted soybean oil present at the interphase between PP and SB particle interphase. Due to its plasticization effect, tensile strength tends to decrease while the percent elongation tends to increase with an increase in SB loading. However, at 2 wt% SB content, %E drastically decreases, reflecting that severe agglomeration of SB particles

is evident. For PP/phosphonated silica composite, an increase in the tensile strength about 20% is achieved with an incorporation of 0.5 wt% - 1.5 wt% silica particles. The corresponding % elongation at break values show the opposite direction. The notable improvement in tensile strength of PP/phosphonated silica composite is found in a similar manner to the previous work<sup>(27)</sup>. This could be interpreted that the particle having rigidity modulus including silica particle is responsible for the tensile property improvement arising from reinforcement effect. In addition, the presence of silica particle in PP matrix causes stiffening effect, resulting in a decreasing percent elongation at break and an increasing modulus. As expected, mechanical properties of ternary composites are found in a good manner with PP/phosphonated silica binary composites. With respect to phosphonated

silica loading content, %E of ternary composites is reversed proportionally with phosphonated silica loading. For an example, at 0.5 wt% phosphonated silica content the composite exhibits drastically reduced (5 folds) elongation at break. When considering tensile strength, this property slightly increases with an increase in phosphonated silica content. The optimum tensile strength of 34.46 MPa is achieved with the addition of 0.5 wt% SB and 1 wt% P, corresponding to 6.8% increase. Impact strength of the ternary composites are presented in Figure 7. From these findings, it could be concluded that soybean oil-g-chitosan exhibits plasticization effect whereas phosphonated silica plays a role in reinforcing composite.

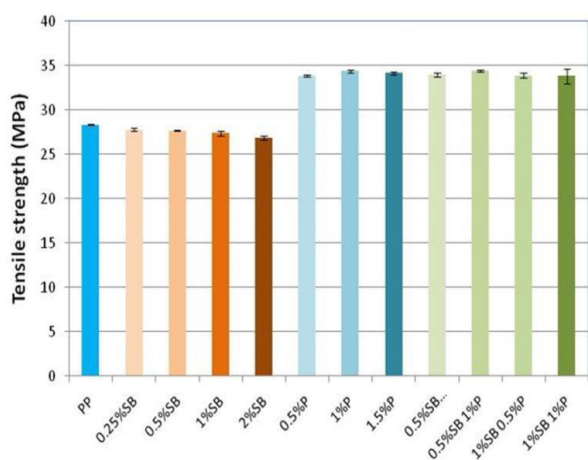


Figure 5. Tensile strength of binary and ternary composites.

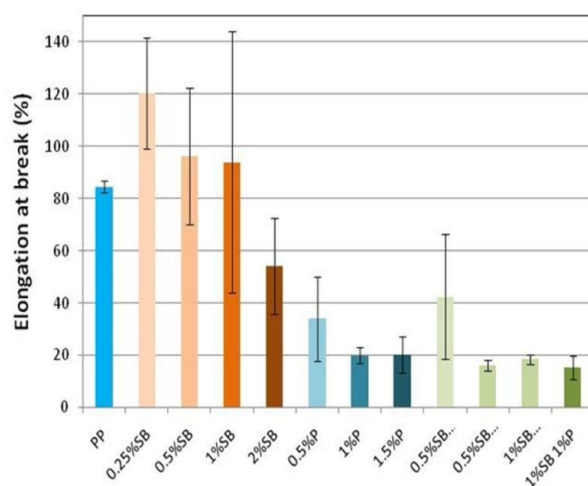


Figure 6. Elongation at break of binary and ternary composites.

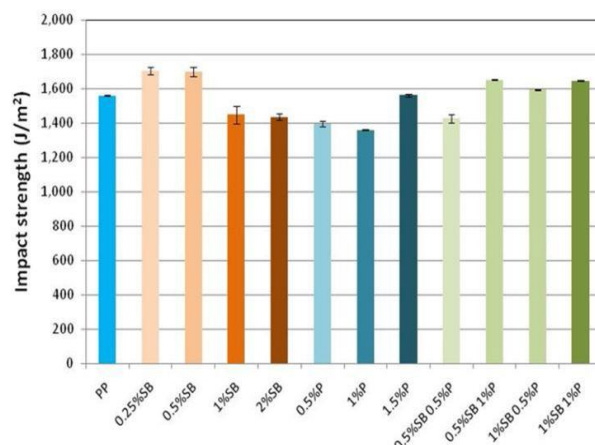


Figure 7. Impact strength of binary and ternary composites.

### Thermal Properties

TGA and DTA results are obtained from the thermogravimetric analyzer. The resultant thermograms are presented in Table 2 and Figure 8-9. PP employed in this experiment exhibits good thermal stability which is indicated by its high  $T_{onset}$  of 301°C. The main degradation occurs at temperatures ranging from 400 to 500°C. For binary and ternary composites, the addition of the phosphonated silica and soybean oil-g-chitosan caused a shift in degradation temperatures of PP which exhibited  $T_d$  of 460°C, indicating that fillers played a role in altering the matrix properties.  $T_d$  values of PP/ 1 wt% SB binary composite, PP/ 1 wt% P binary composite, and PP/ 1 wt% SB / 1 wt% P ternary composite are found at 455°C, 465°C, and 453°C, respectively. According to flame retardancy mechanism, phosphorus and nitrogen containing flame retardants reduce thermal stability of polymer matrix by accelerating the degradation process to form protecting char from further pyrolysis. In case of PP/ 1 wt% SB binary composite, lower thermal stability of PP matrix is observed by its decreasing  $T_d$  value. For PP/ 1 wt% P binary composite, it is interesting to see that the corresponding  $T_d$  value is found higher than that of PP. It is believed that silica particle played a role in improving thermal resistance, hence enhancing thermal properties of the composite<sup>(27)</sup>. However, in the presence of soybean oil-g-chitosan and phosphonated silica, thermal resistance of PP matrix reversely decreases, indicating that thermal stabilizing effect of silica was suppressed by the presence of soybean oil-g-chitosan.

Considering flame retardancy property, phosphonated silica when heated to decomposition temperatures releases an acid. Resultant acid causes the material to form char, a protecting layer which then inhibits the subsequent pyrolysis process. When soybean oil-g-chitosan was filled the residue char at 650°C increased noticeably when compared to neat PP. This indicates that soybean oil-g-chitosan enhanced the formation of char during thermal degradation process. In a combination of phosphonated silica, lower Tonset combined with higher char residue are observed. Extensive discussion of flame retardancy effect is presented in subsequent section.

*Flame Retardancy Properties*

The burning behavior of injected samples was photographed. Burning images are illustrated in Figure 10. It is obvious that molten neat PP drips continuously, indicating fast burning rate of PP due to the absence of flame retardant. For the PP/SB binary composite and PP/P binary composite, burning behavior including relatively slow burning rate and char formation is observed. A decrease in burning rate is indicated by a slow dripping of flaming part as shown in the recorded images. In case of soybean oil-g-chitosan, the chitosan nitrogen groups played a role in forming a char. For phosphonated silica, phosphoric acid produced upon burning underwent condensation reaction to form solid phase or char upon the burning materials. Formed char is thermally decomposed at lower rate than neat PP, hence retarding the diffusion of oxygen supply. The temperature of 30% weight loss (T30) was determined by TGA. Resultant T30 values are presented in Table 2. As found, T30 of neat PP is the lowest at the temperature of 452°C, indicating fast burning rate without char formation due to the absence of flame retardant filler.

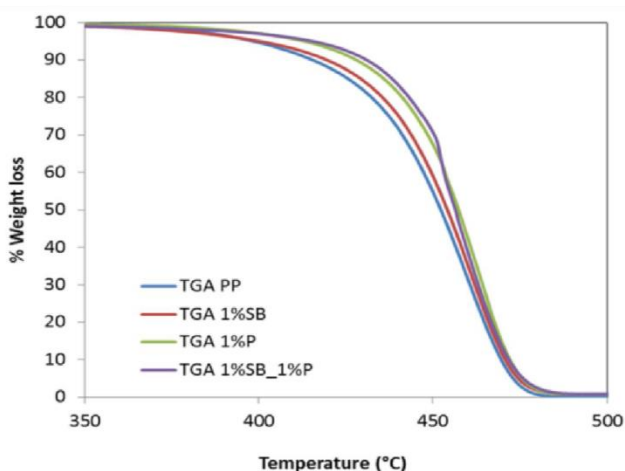


**Figure 8.** TGA thermograms of binary and ternary composites.

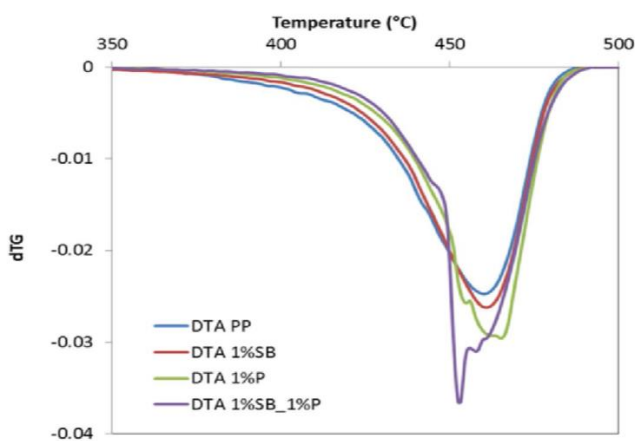


**Figure 9.** DTA thermograms of binary and ternary composites



**Figure 10.** Horizontal burning test of binary and ternary composites containing soybean oil-g-chitosan and phosphonated silica.



**Table 2** Thermal properties of binary and ternary composites

Sample	T <sub>onset</sub> /°C	T <sub>d</sub> /°C	T <sub>30</sub> /°C	lossat 450°C (wt%)	Residue at 600°C (wt%)
PP	350	460	452	45.13	0.07
0.5% SB	317	461	454	40.09	0.11
1% SB	219	463	457	33.86	1.23
1.5% SB	94	464	459	31.02	1.28
0.5% P	133	462	456	34.41	0.24
1% P	82	463	457	33.98	0.72
1.5% P	69	465	457	32.47	0.88
0.5% SB 0.5% P	97	463	454	33.96	0.63
1% SB 1% P	323	453	457	2.249	0.83

*Antimicrobial Activity*

Effect of antimicrobial activity of soybean oil-g-chitosan was evaluated according to method AATCC Test Method 100-1999 using *Staphylococcus aureus*. The percent microbial reduction is presented in Table 3. Also, the antimicrobial activity is presented in terms of viability (Figure 11). A high percent reduction of bacterial colony indicates an antimicrobial activity of a tested sample. The

microbial reduction data from Table 3 indicate that neat PP shows zero antimicrobial activity, indicating that PP has no ability to inhibit growth of microorganism. When considering PP/SB binary composite, the antimicrobial activity against *Staphylococcus aureus* is better than neat PP. This finding provides information that soybean oil-g-chitosan is able to enhance antimicrobial performance of PP composite.

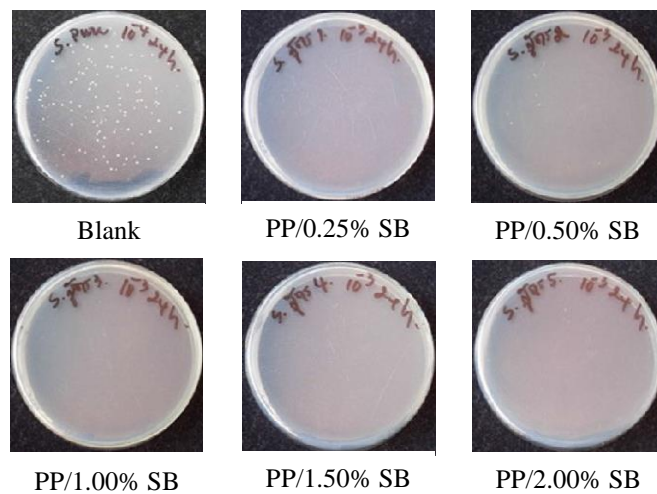


**Figure 11.** Viability test of PP/SP binary composites according to AATCC Test Method 100-1999.

**Table 3** Antimicrobial activity of soybean oil-g-chitosan on *Staphylococcus aureus*

Sample	The number of bacteria CFU/ml (24 h)	% Reduction at
Blank	$1.1 \times 10^7$	-
PP/0.25% SB	0	100
PP/0.5% SB	$5.0 \times 10^4$	99.54
PP/1% SB	0	100
PP/1.5% SB	0	100
PP/2% SB	0	100

## Conclusions

PP/soybean oil-g-chitosan binary composite, PP/phosphonated silica binary composite, and PP/soybean oil-g-chitosan/phosphonated silica ternary composite were prepared and their properties were evaluated. It was found that PP/SB composites exhibited a slight decrease in tensile strength. In the opposite direction, the elongation at break is found higher than that of neat PP due to the plasticization effect of soybean oil-g-chitosan. For PP/phosphonated silica composite, an increase in the tensile strength about 20% was achieved with an incorporation of 0.5-1.5 wt% silica particles. The corresponding % elongation at break values showed the opposite direction. This could be interpreted that silica particles having rigidity modulus was responsible for the tensile property improvement arising from reinforcement effect. Mechanical properties of ternary composites were found in a good manner with PP/phosphonated silica binary composites. The optimum tensile strength of 34.46 MPa was achieved with the addition of 0.5 wt% SB and 1 wt% P, corresponding to 6.8% increase. Young's modulus value of 945.5 MPa was obtained at 0.5 wt% SB and 0.5 wt% P loading, corresponding to 24% higher than neat PP. Burning behavior of binary and ternary composites exhibited slow dripping of flaming part, indicating that soybean oil-g-chitosan as well as phosphonated silica played a role in forming a char, a key player for flame retardancy. Thus formed char was thermally decomposed at lower rate than neat PP. Apart from flame retardancy property, the finding results also showed that soybean oil-g-chitosan was able to provide antimicrobial activity.

## Acknowledgments

The authors would like to thank Ratchadaphiseksomphot Endowment Fund of Chulalongkorn University (RES560530023-AM) and CU Graduate School Thesis Grant.

## References

1. Shubhra, Q.T., Alam, A.K., Gafur M.A., Shamsuddin S.M., Khan, M.A., Saha, M., Dahiya D., Quaiyyum, M.A., Khan, J.A. and Ashaduzzaman, M. (2010). Characterization of plant and animal based natural fibers reinforced polypropylene composites and their comparative study. *Fiber Polym.* **11(5)**: 725-731.
2. Acha, B.A., Roboredo, M.M. and Marcovich, N.E. (2007). Creep and dynamic mechanical behavior of PP-jute composites : Effect of the interfacial adhesion. *Compos. Part A.* **38(6)**: 1507-1516.
3. Unterweger, C., Duchoslav, J., Stifter, D. and Furst, C. (2015). Characterization of carbon fiber surfaces and their impact on the mechanical properties of short carbon fiber reinforced polypropylene composites. *Compos. Sci. Technol.* **108**: 41-47.
4. Jang, B.P., Kowbel, W. and Jang, B.Z. (1992). Impact behavior and impact-fatigue testing of polymer composites. *Compos. Sci. Technol.* **44(2)**: 107-118.
5. Saujanya, C. and Radhakrishnan, S. (2001). Structure development and properties of PET fibre filled PP composites. *Polymer.* **42(10)**: 4537-4548.
6. Omar, M.F., Akil, H.M. and Ahmad, Z.A. (2013). Particle size-Dependent on the static and dynamic compression properties of polypropylene/silica composites. *Mater. Des.* **45** : 539-547.
7. Chan, V., Mao, H.Q. and Leong, K.W. (2001). Chitosan-induced perturbation of dipalmitoyl-sn-glycero-3-phosphocholine membrane bilayer. *Langmuir.* **17(12)**: 3749-3756.
8. Wang, N., Mi, L., Wu, Y., Wang, X. and Fang, Q. (2013). Enhanced flame retardancy of natural rubber composite with addition of microencapsulated ammonium polyphosphate and MCM-41 fillers. *Fire Safety J.* **62**: 281-288.
9. Hu, S., Song, L., Pan, H. and Hu, Y. (2012). Thermal Properties and combustion behaviors of chitosan based flame retardant combining phosphorus and nickel. *Ind. Eng. Chem. Res.* **51(9)**: 3663-3669.
10. Scharrel, B. (2010). Phosphorus-based flame retardancy mechanisms-old hat or a starting point for future development?. *Materials.* **3(10)**: 4710-4745.

11. Gallo, E. (2009). *Progress in polyesters flame retardancy new halogen-free formulations*. Ph D Dissertation, UNINA, Naples
12. Manias, E., Polizos, G., Nakajima, H. and Heidecker, M.J. (2007). *Fundamentals of polymer nanocomposite technology*. John Wiley & Sons, New Jersey. p. 31-66.
13. Hamada, M. and Yasuda, S. (1982). *Flame retardant silicone rubber compositions containing carboxamides*. U. S. Patent. No. 4366278A.
14. Qian, L., Ye, L., Qiu, Y. and Qu, S. (2011). Thermal degradation behavior of the compound containing phosphaphenanthrene and phosphazene groups and its flame retardant mechanism on epoxy resin. *Polymer*. **52(24)**: 5486-5493.
15. Du Pont De Nemours, E.I. and Company. (2012). *Compositions élastomères thermoplastiques de copolyester ignifugeantes sans halogène, stables à la chaleur*. W. O. Patent No. 2012024280A1.
16. Sandler, S.R. (1980). *Polyamide resins flame retarded by poly(metal phosphinate)s*. U. S. Patent No. 4208321A.
17. Chen, J., Liu, S. and Zhao, J. (2011). Synthesis, application and flame retardancy mechanism of a novel flame retardant containing silicon and caged bicyclic phosphate for polyamide 6(J). *Polym. Degrad. Stabil.* **96(8)**: 1508-1515.
18. Gui, H., Zhang, X., Liu, Y., Dong, W., Wang, Q., Gao, J., Song, Z., Lai, J. and Qiao, J. (2007). Effect of dispersion of nano-magnesium hydroxide on the flammability of flame retardant ternary composites. *Comp. Sci. Technol.* **67(6)**: 974-980.
19. Kashiwagi, T., Shields, J.R., Harris, R.H., Jr. and Davis, R.D. (2003). Flame-Retardant Mechanism of Silica : Effects of Resin Molecular Weight. *J. Appl. Polym. Sci.* **87(9)**: 1541-1553.
20. Gilman, J.W. (1999). Flammability and thermal stability studies of polymer layered-silicate (clay) nanocomposites. *App. Clay Sci.* **15(1-2)**: 31-49.
21. Kiangkitiwan, N. and Srikulkit, K. (2013). Poly(Lactic Acid) filled with cassava starch-g-soybean oil maleate. *Sci. World J.* **2013**: 1-7.
22. Punyacharoenon, P., Charuchinda, S. and Srikulkit, K. (2008). Grafting and phosphonic acid functionalization of hyperbranched polyamidoamine polymer onto ultrafine silica. *J. Appl. Polym. Sci.* **110(6)**: 3336-3347.
23. CLSI, *Methods for dilution antimicrobial susceptibility tests for bacteria that grow aerobically : approved standard-Eighth Edition*. CLSI document M07-A8, 2009.
24. Junaidi, M., Khoo, C.P. and Ahmad, A.L. (2014). The effects of solvents on the modification of SAPO-34 zeolite using 3-aminopropyl trimethoxy silane for the preparation of asymmetric polysulfone mixed matrix membrane in the application of CO<sub>2</sub> separation. *Micropor. Mesopor. Mat.* **192**: 52-59.
25. Jung, H.Y., Gupta, R.K., Oh, E.O., Kim, Y.H. and Whang, C.M. (2005). Vibrational spectroscopic studies of sol-gel derived physical and chemical bonded ORMOSILs. *J. Non-Cryst. Solids.* **351(5)**: 372-379.
26. Srisawat, N., Nithithanakul, M. and Srikulkit, K. (2011). Spinning of fibers from polypropylene/silica composite resins. *J. Compos. Mater.* **46**: 99-110.